IOP Publishing Nanotechnology

Nanotechnology **27** (2016) 105201 (11pp) doi:10.1088/0957-4484/27/10/105201

Theoretical study of carbon-based tips for scanning tunnelling microscopy

C González[1,2], E Abad[3], Y J Dappe[1] and J C Cuevas[4]

[1] SPEC, CEA, CNRS, Université Paris-Saclay, CEA Saclay 91191 Gif-sur-Yvette Cedex, France
[2] Departamento de electrónica y Tecnología de Computadores, Universidad de Granada, Fuente Nueva & CITIC, Aynadamar E-18071 Granada, Spain
[3] German Research School for Simulation Sciences GmbH 52425 Jülich, Germany
[4] Departamento de Física Teórica de la Materia Condensada and Condensed Matter Physics Center (IFIMAC), Universidad Autónoma de Madrid, E-28049 Madrid, Spain

E-mail: cesar.gonzalez.pascual@gmail.es

Received 3 September 2015, revised 1 December 2015
Accepted for publication 14 January 2016
Published 10 February 2016

Abstract

Motivated by recent experiments, we present here a detailed theoretical analysis of the use of carbon-based conductive tips in scanning tunnelling microscopy. In particular, we employ *ab initio* methods based on density functional theory to explore a graphitic, an amorphous carbon and two diamond-like tips for imaging with a scanning tunnelling microscope (STM), and we compare them with standard metallic tips made of gold and tungsten. We investigate the performance of these tips in terms of the corrugation of the STM images acquired when scanning a single graphene sheet. Moreover, we analyse the impact of the tip-sample distance and show that it plays a fundamental role in the resolution and symmetry of the STM images. We also explore in depth how the adsorption of single atoms and molecules in the tip apexes modifies the STM images and demonstrate that, in general, it leads to an improved image resolution. The ensemble of our results provides strong evidence that carbon-based tips can significantly improve the resolution of STM images, as compared to more standard metallic tips, which may open a new line of research in scanning tunnelling microscopy.

Keywords: STM, graphene, DOS, simulations

(Some figures may appear in colour only in the online journal)

1. Introduction

Since the first scanning tunnelling microscope (STM) was built by Binnig and Rohrer more than 30 years ago [1], it has been successfully used for the characterisation and study of the atomic and electronic structure of a great variety of surfaces: semiconductors, metals, and all kinds of adsorbed atoms and molecules (some examples can be found in [2–6]). In most of these works, theoretical calculations complemented the experimental measurements, improving the understanding of the system under study. In the early days of the STM theory, the common approximation, the so-called Tersoff–Hamman approach, only took into account the electronic structure of the surface, whereas the tip was simply considered as an *s*-orbital [7, 8]. However, this basic model turned out to be insufficient to explain many of the experimental images. Some years later, Chen's approximation generalised the initial model for *p*-orbitals [9]. Later on, new models were developed to properly include the complete electronic density of states (DOS) and geometry of the tip [10–12], allowing for an explanation of the obtained images for complex situations such as contrast changes [3, 13, 14].

The measurements in the context of STM are usually performed with metallic tips made of W, Au, Pt or Ir. In recent years, and in order to improve the resolution of the STM images, many groups have investigated the possibility of attaching different atoms/molecules in the apex of the standard tips. Thus for instance, Bartels and coworkers studied how a CO molecule can be adsorbed to the STM tip and showed how the CO-functionalised tip produced a contrast change in the STM image of CO molecules adsorbed on a metallic surface [15, 16]. Some years later, Gross

et al showed that these CO-contaminated tips are able to resolve the molecular structure of a pentacene with either an atomic force microscope or an STM [17, 18].

Another study was performed by Weiss and coworkers [19, 20] showing that the resolution of STM images of a PTCDA molecule deposited on a metallic surface, taken with a gold tip, could be greatly improved upon the introduction of H_2 molecules in the chamber. These authors suggested that one H_2 molecule was placed in between the Au tip and the molecule producing a crucial change in the tip-molecule current that resulted in an improved resolution. Based on density functional theory (DFT) calculations, some of us concluded that this situation is not stable and that the H_2 molecules are indeed dissociated by the gold-apex of the tip [21]. The resulting H-atoms are then adsorbed in the gold tip leading to a modified charge distribution in the last atoms. This fact results in a higher weight of the *p*-orbitals on the metallic apex, which enables the PTCDA hexagons to be resolved in the simulated STM images.

Other tip-contaminants such as oxygen atoms or molecules have also been explored [3, 14, 22]. The replacement of the final metallic apex in a Pd tip by one single O atom changes the contrast in the system O/Pd(111) analysed in [3]. When the tip presents a metallic atom, the oxygen atoms adsorbed on the surface appear as protrusions in the STM image, while they appear as depressions when a contaminated O-tip is used. On the contrary, an O atom in the apex of a W tip does not change the image contrast when it is applied over a rutile TiO2-(1x1) surface. The reason is the great affinity between the Ti atoms (observed in the STM image) and the O in the apex [14].

In recent years, researchers have been searching for new conducting tips beyond the standard metallic ones. In this respect, different kinds of carbon-based tips have been proposed as promising STM tips that could improve the resolution of the images. Thus for instance, diamond tips have proved their capability to produce atomic resolution on graphite [23]. The results presented in that work were explained in terms of the *p*-orbitals of last carbon atoms in the tip. As such, the maximal tunnelling current is obtained when the tip is placed on top position over a carbon atom of the graphite. Following this idea, very recently Li and coworkers showed that a tungsten tip functionalised with Cl can improve the resolution in an ultrathin layer of NaCl deposited over a Au (111) surface and it can lead to a contrast reversal in the STM image [13]. Both changes were attributed to the strong *p* character of the Cl apex. On the other hand, different experiments using carbon fiber tips have obtained atomic resolution [24–27]. Recent experiments performed by Castellanos–Gómez *et al* showed the ability of the carbon fiber tips to reproduce the characteristic triangular and hexagonal images on graphite [27]. Some of us addressed these experiments by simulating a graphitic-like tip decorated with H-atoms [28]. We demonstrated that atomic resolution of surfaces such as Au(111) or a single graphene layer can be obtained with this tip.

In this work, we present a thorough theoretical analysis of different carbon-based tips used in STM. In particular, we present a comparative study between the performance of these tips and the more standard metallic tips. As a prototypical system, we report here STM images of a single graphene sheet acquired with the different investigated tips. In our study, we pay special attention to the role of tip-contaminants on the resolution of the images. Moreover, we also investigate the relevance of the tip-sample distance at which the STM operates and show that it has a strong impact in both the corrugation and symmetry of the images. Overall, our results clearly suggest that carbon-based tips provide a better image resolution as compared to standard metallic tips, which provides a new avenue for scanning tunnelling microscopy.

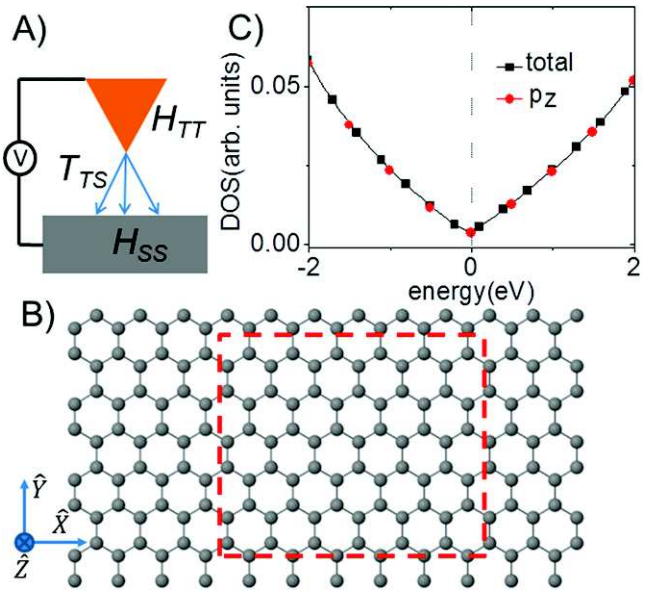

Figure 1. (A) Schematic diagram of the STM microscope, (B) atomic geometry of the graphene (the blue arrows indicate the three $\hat{X}$, $\hat{Y}$ and $\hat{Z}$ directions) and (C) the DOS of one C-atom showing its p_z contribution.

2. Model and method of calculation: relaxation of the different tips and STM calculation

All the theoretical simulations of the STM current and images presented in this work are based on non-equilibrium Green function techniques [10, 31]. In this method, the whole system is described by a Hamiltonian that can be divided into three independent parts (see figure 1(A)): tip (T), sample (S) and tip-sample interaction ($T_{TS/ST}$). The tip and the sample are treated separately and the information on their respective electronic structures, or more precisely on their DOS ρ_{TT} and ρ_{SS}, enters into the current calculations via the following expression obtained at zero temperature

$$I = \frac{4\pi e^2}{h}\int_{E_F}^{E_F+eV} \mathrm{Tr}\,[T_{TS}\rho_{SS}(E)D^r_{SS}(E)T_{ST}\rho_{TT} \times (E-eV)D^a_{TT}(E-eV)]\,\mathrm{d}E. \quad (1)$$

Here, V is the applied bias voltage and E_F is the Fermi energy. The complex matrices D^a_{TT} and D^r_{SS} are directly related to the

Table 1. Cutoff radii in atomic units for the different elements used in this work.

	r_c(a.u.)			
	H	C	O	Au
s	4.1	4.5	3.3	4.5
p	-	4.5	3.8	4.9
d	-	-	-	5.3

multiple scattering (MS) effect produced by the possible electronic reflexions that could take place when the tip is close to the sample. For normal tunnelling distances (between 5 and 7 Å), these matrices tend to the identity, simplifying the final equation. We will take into account these MS effects for distances below 4.5 Å where the image contrast can change drastically, as has been previously noted on graphite [30]. A detailed description of our approach can be found in [32].

In order to use equation 1 we need to obtain the DOS for both isolated systems. For this purpose, we have first optimised the geometry of the tip and sample separately with the FIREBALL code [33]. Based on the DFT technique, the FIREBALL code is a very efficient tool that uses the local density approximation for the exchange and correlation functional following the McWeda approach [34] and a combination of atomic-like orbitals as a basis set. Each orbital decays to zero for a defined cutoff radius (r_c) [35]. In table 1, all the corresponding values for the different orbitals of the elements used in this work are shown in atomic units. The sample chosen in this work is a single graphene layer, represented by a 6×6 superficial unit cell (the area inside the red rectangle in figure 1(B). The simulation was performed using 1024 k-points in the first Brillouin zone and a vacuum in the perpendicular direction of 50 Å. The resulting C-C distance was 1.43 Å, close to the value for a sp^2 hybridisation (1.42 Å) as explained in [36] and obtained experimentally [39]. Then, the Hamiltonian (H_{SS}) is extracted in order to obtain the complete density matrix:

$$\rho_{SS}(\epsilon) = -\frac{1}{\pi}\mathrm{Im}(\mathbb{I}(\epsilon + i\eta) - H_{SS})^{-1}, \qquad (2)$$

where $\mathbb{I}$ is the identity matrix, ϵ is the energy, and η corresponds to a small imaginary part of the energy ($\eta = 0.05$ eV in our calculations). The η parameter is used in a contour integration of the Green functions in the complex plane inducing a finite width in the levels of the Hamiltonian (see below the implication on the cluster tips). In figure 1(C), the total DOS for a C-atom is shown, reflecting the (almost) total p_z contribution around the Fermi level. This result is consistent with previous DOS found in the literature [37, 38].

The second subsystem that we need to optimise for the STM simulation is the tip. In this work, we consider two different families: metallic tips made of gold, and carbon-based tips, including graphitic and diamond-like tips. The gold tip is built using four layers of the fcc Au(111) with a 5×5 periodicity coupled to a pyramid cluster of four gold atoms, as shown in figure 2(A). Then, the tip is ended by a

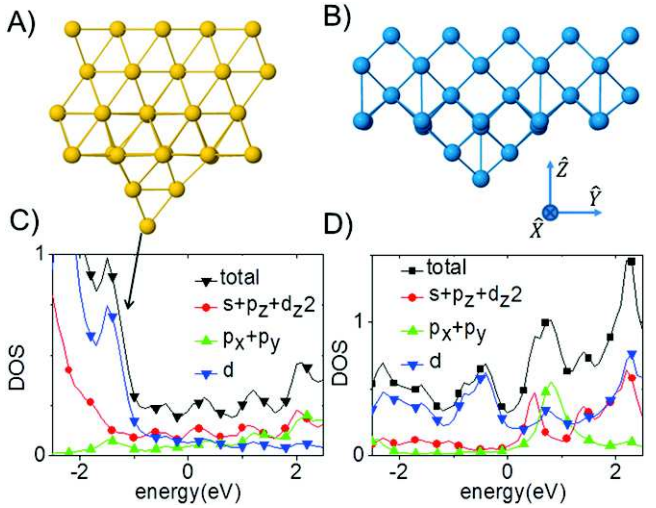

Figure 2. (A) and (B) Atomic geometry of the clean Au-tip and W-tip respectively (the blue arrows indicate the three $\hat{X}$, $\hat{Y}$ and $\hat{Z}$ directions). (C) and (D) total DOS of the gold and tungsten apex (black squares) respectively, together with different contributions: $s + p_z + d_{z^2}$ orbitals (red circles), $p_x + p_y$ (green up triangles) and the other four d orbitals (blue down triangles).

single metallic atom where other atoms or molecules (H or CO) can be adsorbed. In order to check the influence of the metal and the crystal structure, a W-tip has been built as shown in figure 2(B). Following the same methodology we have created four layers of bcc tungsten in its preferential orientation, the (110). Due to the different atomic configuration, now the pyramid is formed by five atoms. Each tip is relaxed using 16 k-points in the first Brillouin zone until the forces are less than 0.05 eV $Å^{-1}$, maintaining the last two layers fixed. The resulting DOS projected onto the most relevant atoms of both tips have been calculated from equation 2 using the tip Hamiltonian. The DOS for the gold and tungsten tips are depicted in figures 2(C) and (D), respectively. The metallic apex presents a complex distribution of the DOS around the Fermi level (set to $E_F = 0$ eV) in both cases. We have separated the total DOS (black squares) in three different contributions: the sum of the directional orbitals s, p_z and d_{z^2} (red circles), the perpendicular p orbitals (p_x and p_y) represented by green up-triangles and the other four d orbitals (blue down-triangles). While the three contributions have a similar magnitude around the Fermi level in the gold tip, a predominant d character is found in the tungsten apex associated with the half filled shell.

Secondly, the graphitic tips were built as previously reported in [28]. The atomic configuration is shown in figure 3(A): three triangular graphene-like layers saturated with H at the edges. In the figure, only one flake is shown, the other two being shorter and placed in the corresponding graphitic positions. The tunnel current comes mainly from the atoms in the central flake. In order to compare to a more standard amorphous carbon-tip (trying to mimic the current experimental C-based tips), we have removed the H atoms of this graphitic tip, leaving the C atoms to reach the most comfortable configuration. For that purpose, the molecular

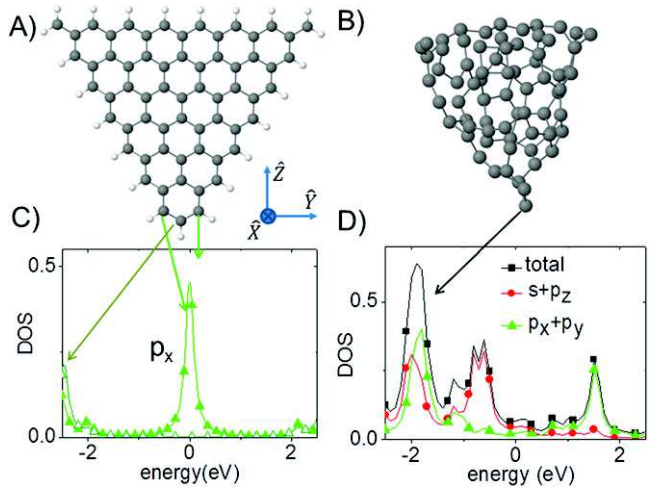

Figure 3. (A) and (B) Atomic geometry of the graphitic and amorphous tips respectively (the blue arrows indicate the three $\hat{X}$, $\hat{Y}$ and $\hat{Z}$ directions). (C) p_x contribution to the DOS of the last three C-atoms in tip A). (D) Total DOS of the C apex (black squares) together with different contributions: $s + p_z + d_{z^2}$ orbitals (red circles), $p_x + p_y$ (green up triangles) and the other four d orbitals (blue down triangles).

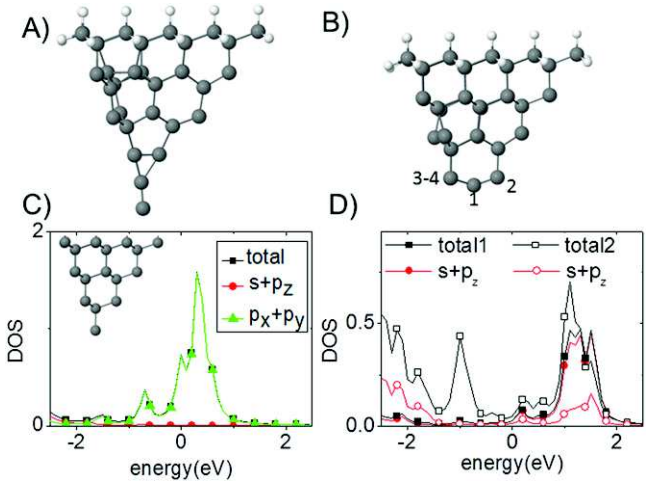

Figure 4. (A) and (B) Atomic geometry of the diamond tips used in this work. The last C atom in (A) has been removed to obtain the (B) tip. (C) and (D) the corresponding total DOS of the C apex (black squares) for the tips shown in A) and B) respectively, together with their different contributions: $s + p_z$ orbitals (red circles) and $p_x + p_y$ (green up triangles). The inset in (C) shows the ideal diamond tip before relaxation. A similar tip was used in [23].

dynamics (MD) technique implemented in the FIREBALL code is used to ease the process. Firstly, we have started the MD calculation for different temperatures leaving the atoms to move freely for several hundred of steps, except the top-most atoms of the central slide that remained fixed. After that, the MD calculation is stopped and the system is optimised. The most stable configuration obtained with this procedure presents a single C-apex as shown in figure 3(B). We did not include any periodicity in the tips, so they have been relaxed as a cluster using only the Γ point, maintaining the last atoms of each tip fixed and following the same tolerance criteria as before. The effect of a semi-infinite electrode below the cluster should induce a broadening in the energy states of the atoms of the tip. The width can be compensated by the inclusion of a slightly larger value of η in the DOS calculation. For the cluster tips, η is fixed to 0.1 eV. The DOS for both tips are depicted in figures 3(C) and (D), respectively. Interestingly, in the graphitic tip, the last C atom presents a gap of more than 4.0 eV, while the following two C atoms in the last hexagon exhibit a peak at the Fermi level due to the half-filled p_x band. Note that this band corresponds to the $p_z$bond in the graphene layer below. This peculiar DOS distribution produces an hexagonal pattern in the STM simulations over graphene, as shown before in [28]. We have checked that the same DOS curves are obtained when a periodicity is imposed in the Y-direction (see the directions in the figure). The DOS of the amorphous C-tip have been separated in a similar way as the metallic cases. The total DOS is represented by black squares and it is decomposed in two contributions: on one hand the orbitals s, p_z(red circles), and on the other hand the perpendicular p orbitals (p_x and p_y) represented by green up-triangles. Now both contributions have a similar planar magnitude above the Fermi level suggesting that this tip could be useful for dI/dV spectroscopy.

Finally, the diamond tip is presented in figure 4(A). We have built a cluster formed by 55 C atoms following the diamond structure shown by Grushko *et al* [23]. The bonds of the atoms in the last layer are saturated with 30 H atoms. Thus, the tip is relaxed with the Γ point using the same conditions explained for the previous cluster tips. The unrelaxed tip (shown in the inset of figure 4(C)) is similar to the one previously presented in [23]. An alternative tip is created by removing the C-atom at the apex, whose corresponding optimised geometry is shown in figure 4(B). The DOS projected onto the last C-atom of figure 4(A) is shown in the C) panel. The main contribution around the Fermi energy comes from the p_x and p_y orbitals. On the other hand, when this last atom is removed, two C atoms, labelled with 1 and 2 in the atomic structure, have a significant contribution to the DOS around the Fermi energy coming from the s and p_z orbitals (see figure 4(D)). The DOS analysis suggests that both tips have a different behaviour in the STM images, as confirmed below.

After that, as we will describe in more detail below, we have also investigated variations of the tips described above that were decorated by the addition of different kinds of atoms or molecules. For example, we have investigated the gold tip decorated with one (or four) H atoms and one CO molecule adsorbed at the apex. In the case of the graphitic tip, we removed the last H atom or replaced it by an O atom or an OH group. Similarly, the diamond tips have been contaminated with one O atom or an OH group. In the following section, we shall discuss the electronic and geometrical effects in the resolution of the STM images calculated with the different tips.

The last terms of equation 1 are related with the tip-sample coupling (the matrices $T_{TS/ST}$). We estimate them

using the dimer approximation. Firstly, a dimer formed by an atomic specie from the tip and one atomic specie from the substrate can be created for a large range of distances (in our case from 2 to 15 Å, atoms at larger distances do not have an important contribution in the current). Secondly, all the important interactions ($ss-\sigma$, $sp-\sigma$, $pp-\sigma$, $pp-\pi$, ...) for all the mentioned distances are tabulated in one database file that the code can read during the calculation. Considering the distance and the relative position of the atoms, the code interpolates and rotates the different interactions to create one atom–atom interaction matrix. This is done for all the possible combinations of atoms between the tip and the sample to finally obtain the complete $T_{TS/ST}$ matrixes. Again the Hamiltonian is created with the FIREBALL code and the orbitals' cutoff radii have been increased in order to cover the whole range of distances mentioned before. This means that the interaction matrices change at each point of the STM simulation, contrarily to the DOS of the tip and graphene that remain unperturbed during the calculation. This approximation has been successfully used in many works before [2, 3, 14, 28, 30].

3. Results: relation between tip geometries, DOS and the STM images

In this section, we present the STM images obtained for a tip-graphene distance of 4.5 Å and applying a small bias ($V_S = -0.1$ V) (except in the indicated cases) with the different tips analysed in this work and we make the connection between the geometry and DOS of the apex atoms. We divide our tips into two main families, namely metallic tips and carbon-based tips, including graphitic, amorphous and diamond-like tips. We mainly focus on the atomic resolution of the corresponding STM images and the corrugation obtained with each tip model. It is important to notice that within our methodology the current is usually overestimated, while the corrugation is underestimated compared to the experimental values, as was previously explained [14].

3.1. Clean tips

Let us start with the clean cases, i.e. the tips presented in the methodology section: two standard metallic tips made of gold and tungsten (see figures 2(A) and (B)), a graphitic tip (figure 3(A)), an amorphous C-tip (figure 3(B)) and the two different diamond tips shown in figures 4(A) and (B).

3.1.1. Metallic tips. In figures 5(A) and (B) the graphene STM images calculated with a gold tip are presented for short (3 Å) and large (4.5 Å) distances respectively. Both contrasts have been previously observed experimentally [39]. In the first case, the image has a triangular pattern with the current maxima located over the hollow positions, while in the second case the current maxima are placed over the atoms resulting in the characteristic honeycomb pattern of graphene. This change of the image contrast has already been previously suggested theoretically for graphite [30]. In the third panel

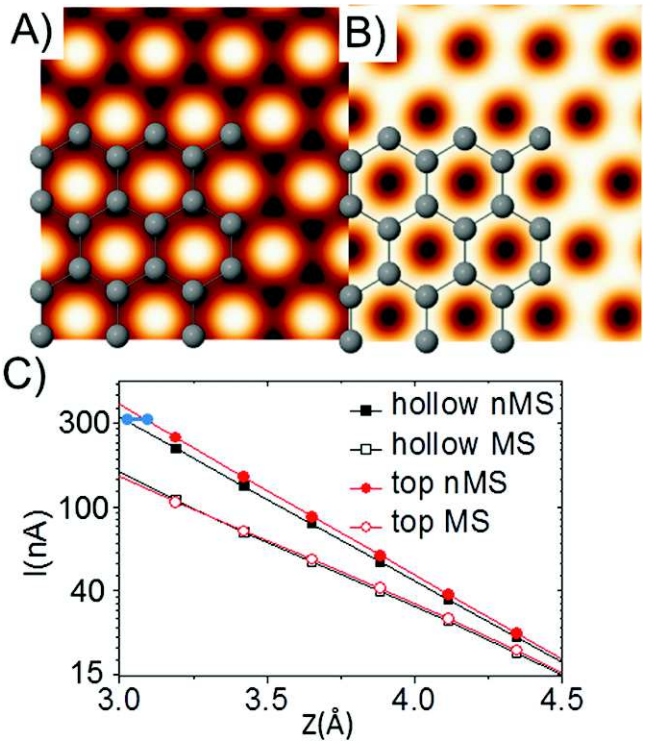

Figure 5. Calculated STM images obtained with our gold tip: (A) triangular pattern with the maxima over the hollow positions obtained at 3.0 Å and (B) honeycomb pattern and atomic resolution at 4.5 Å. (C) I(Z) curves calculated over a C atom (red circles) and a hollow position (black squares) with/without the inclusion of the MS effects (open/filled symbols). The change between the hexagonal and triangular regime is produced at a tip-sample distance of 3.35 Å. The blue line defines the way the corrugation is estimated. The WSxM software has been used to plot the STM images [40].

(figure 5(C)), we show the calculated current for different tip-sample distances (defined as the distance between the metallic apex and the graphene layer) with and without the inclusion of the MS effects previously explained in section 2. The filled symbols correspond to the simulations without the MS. It is important to notice that, when the MS effects are not taken into account, the current over the C atom is higher than on the hollow site for all distances. This means that the directional $s + p_z + d_{z^2}$ orbitals give the main contribution to the tunnelling current. This is in agreement with the DOS presented in figure 2(C) for the energies around the Fermi level. Notice that the DOS involved in the simulation falls inside the interval [0, +0.1] eV corresponding to the voltage $V_S = -0.1$ V applied to the graphene layer. With the inclusion of the MS effects, a different behaviour is found. The I(Z) curves show a contrast change for a tip-sample distance of around 3.35 Å. In this case, the MS produces a current saturation over the C atoms due to the electronic reflexions established between the tip and the graphene layer, leading to a maximum on the hollow site. On the other hand, for larger distances the current converges to the values without MS effects (when the D^a_{TT} and D^r_{SS} matrices tends to the identity in equation 1). The curves in figure 5 illustrate the importance of taking the MS effects in the image simulations

especially for distances below 4 Å. For this reason, we will include them in the following calculations. Notice that for very short distances, the tip-sample interaction could generate atomic deformations in both subsystems (tip and graphene) and consequently the STM image could change again. We did not take this effect into account in our analysis, and for this reason we have restricted our attention to tip-sample distances larger than 3 Å.

In order to quantify the resolution of an STM tip, we need to estimate the corresponding corrugation for different tip-sample distances. Maintaining a constant current in an STM image, the corrugation is defined as the difference between the height of the maximum and the minimum. Drawing a line parallel to the z-axis in figure 5(C) (see the blue line), we can measure the value of the corrugation for a chosen current value by subtracting the heights for both hollow and top sites. A closer look at the curves near 4.5 Å reveals that the corrugation is very low (around 0.02 Å for a current of 15 nA). This poor result justifies the interest in new tips that could improve the resolution increasing the corrugation.

Similar results can be obtained for the W tip shown in figure 2(B): the corrugation estimated at a distance of 4.5 Å is similar to the value obtained for the gold tip and a contrast change is obtained when the tip is approached to the graphene monolayer. For this reason, we will analyse only the decorated Au-tips in the following sections. Now, the contrast change is produced at a larger distance (3.70 Å) close to the value previously obtained for graphite [30]. Interestingly, the current at 4.5 Å has decreased to 3.7 nA (with the gold tip the value was 15 nN). Both effects can be explained by the higher weight of the non-directional d-orbital in the DOS of the apex, reducing the current over the C atoms while it raises on the hollow sites as the tip-graphene distance is getting closer.

3.1.2. Graphitic and amorphous carbon tips. We now consider carbon-based tips, starting with the graphitic model previously used for molecular electronics modelling [28] and shown in figure 2(B). In this case, we also obtain atomic resolution (see figure 6(A)), but the images depend on the exact relative orientation between the tip and the surface. In figures 6(B) and (C) the STM images are shown for two different tip orientations. In the three images a ball and stick model of the graphene is superimposed on the STM images together with three black spheres representing the last C atoms of the tip. In figure 6(B), a triangular-like pattern is observed, while in figure 6(C) an asymmetric hexagonal image is obtained. This first one is a good example of the fact that an STM image does not only consist in the mapping of the electronic density of the sample, but that it is a convolution between the DOS of the tip and the DOS of the sample. In particular, this image originates from the high anisotropy of the p_x orbital of two C atoms perpendicular to the tip plane (see the huge contribution shown in figure 2(D)), which provides the most important contribution to the STM current. Indeed, since all the carbon atoms are saturated with H atoms, the only potentially interacting orbital is the out-of-plane p_x parallel to the surface of the two atoms. When the tip falls over the graphene layer with the relative orientation shown in figure 6(A), the interaction between the p_x orbitals from the tip and the p_z orbitals from the graphene layer is optimised at certain points producing the honeycomb pattern. On the contrary, with the orientation of figure 6(B), the optimisation is strong in a very small region (in the center of the C-C bonds formed along the $\hat{Y}$-direction) giving the triangular shape to the image. The intermediate case is shown in figure 6(C) where the hexagonal pattern is recovered but with asymmetric maxima due to the slightly different relative positions of the C atoms of the tip versus the atoms in the graphene sheet. Notice that in all the cases, both maxima and minima are displaced from the common top and hollow positions. These results show the influence on the STM image of the electronic and geometrical properties of the tip.

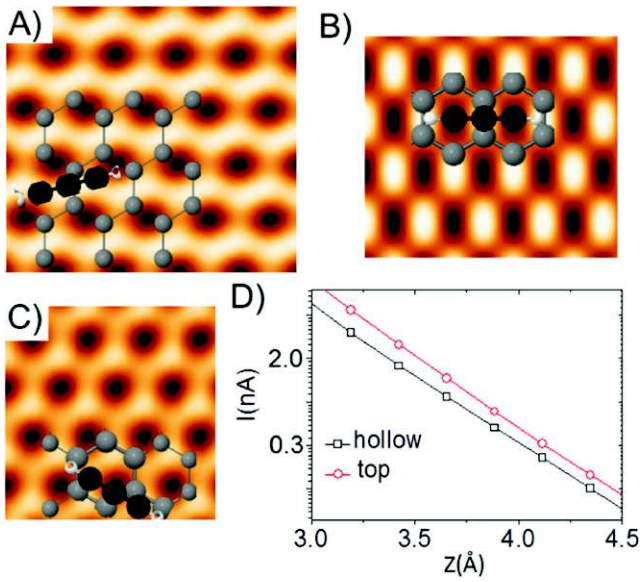

Figure 6. Calculated STM images obtained with our graphitic tip (placed at 4.5 Å) for three different relative orientations related to the graphene layer and indicated in the corresponding superimposed ball and stick models (black spheres represents the tip atoms). (A) Shows a honeycomb pattern, (B) a triangular-like pattern and (C) a hexagonal pattern with two asymmetric maxima. (D) I(Z) curves calculated including the MS effects over a maximum (red circles) and a depression (black squares) of the STM image shown in (A). The image remains unchanged with this tip.

In figure 6(D), the corresponding I(Z) curves are obtained when the tip is oriented as shown in panel (A) and it falls over the maximum and the minimum points. The first important difference when comparing with the gold tip is the lower current obtained, more than two orders of magnitude. The second important difference is that for this tip there is no contrast change (at least in the range of tip-sample distances explored in this work). Taking as a reference the highest current obtained at 4.5 Å (0.09 nA), the corrugation is 0.10 Å confirming a higher resolution than the gold tip. If the tip is moved down in order to obtain the same reference current than with the metallic tip, the resulting corrugation grows to 0.15 Å. We would like to stress an additional advantage of

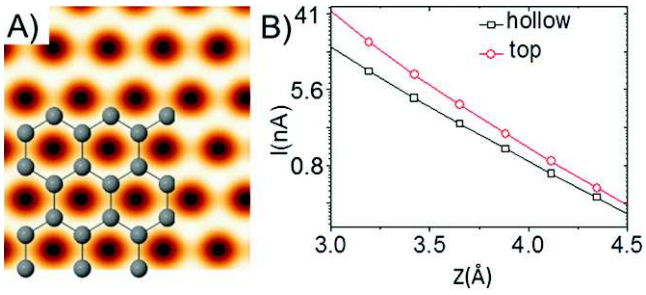

Figure 7. (A) Calculated STM image obtained with the amorphous carbon tip (placed at 4.5 Å) showing a honeycomb pattern (the atomic structure of the graphene is superimposed), (B) I(Z) curves calculated including the MS effects over an atom (red circles) and a hollow site (black squares) of the STM image shown in (A). The image remains unchanged with this tip.

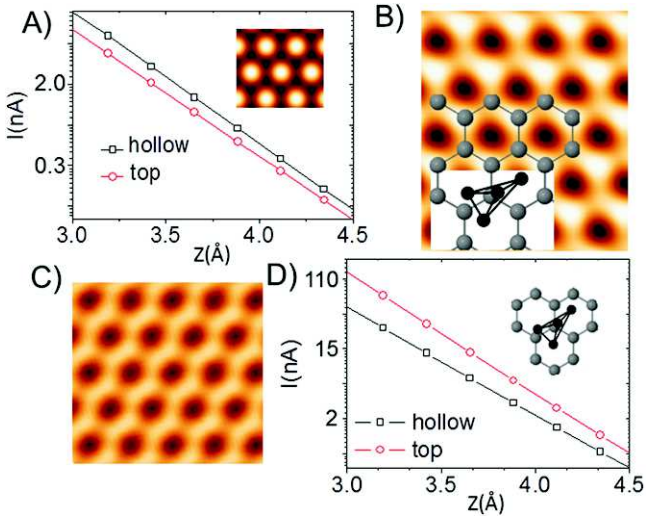

Figure 8. (A) I(Z) curves calculated for the diamond tip shown in figure 4(A) over a C atom (red circles) and a hollow position (black squares) including the MS effects. In the inset, the calculated STM image shows the maxima in the hollow positions. (B) Calculated STM image obtained with the diamond tip presented in figure 4(B) for the orientations related to the graphene layer indicated in the superimposed ball and stick models (the black spheres represent the tip atoms). The image shows an asymmetric hexagonal pattern. (C) STM image exhibiting a symmetric hexagonal or honeycomb pattern when the same tip is rotated 15 degrees as shown in the inset in (D), where the corresponding I(Z) curves shown have been calculated including the MS effects over a maximum (red circles) and a depression (black squares).

this tip: it is poorly reactive, allowing contact experiments in a non-invasive way.

Figure 7(A) shows the STM image calculated at a distance of 4.5 Å with the amorphous carbon tip presented before. Now the maxima over the C atoms have been recovered as is shown by the graphene structure superimposed. This is explained by the single C apex in the tip and its important contribution of the directional orbitals in the DOS presented in figure 3(D). Doing a vertical scan over both top and hollow positions, we found that as happened previously with the graphitic-tip, there will be no contrast change in the STM image for shorter tip-graphene distances (see the I versus Z curves of figure 7(B)). Now at 4.5 Å, the current is slightly larger (0.25 nA) than with the graphite tip, but the corrugation is estimated in 0.08 Å, slightly lower than the previous tip. If we move the tip closer to the graphene layer until the reference value of the gold tip is obtained (15 nA), the value of the corrugation grows to 0.21 Å at a distance of 3.3 Å. It means that this tip offers better resolution than the graphitic tip when it is close to the contact regime. Nevertheless, we will decorate only the graphitic tip due to the expected similar behaviour of the amorphous tip with the diamond tips proposed in the following section.

3.1.3. Diamond tip. We now turn to the last type of carbon-based tips, which is diamond-like carbon tips, following the model of Grushko *et al* [23] and shown in the inset of figure 4(C). The STM image shown in the inset of figure 8(A) is calculated with the relaxed tip presented in figure 4(A). The image presents a triangular pattern, with the maximum value in the hollow position. The I(Z) curves calculated over a C-atom and a hollow position in figure 8(A) show that the triangular shape is obtained for all the calculated distances. The explanation can be found in the dominant contributions of the anisotropic p_x and p_y orbitals of the apex that maximises the tip-sample electronic hopping with the C-p_z orbitals of the graphene sheet when the tip is placed over the hollow site.

When the last C atom is removed the final four C-atoms are rearranged as shown in figure 4(B). The DOS projected onto the atoms labelled 3 and 4 have a gap around the Fermi level. On the other hand, the atoms 1 and 2 have a contribution of the $s + p_z$ orbitals as shown in figure 4(D). In figures 8(B) and (C) the STM image is shown for two different orientations of the tip with respect to the graphene layer. In the first case, an asymmetric hexagonal image is obtained, in a similar way as the graphitic tip of figure 6(C) presented before. The brightest spot is obtained when the 1 and 2 C atoms from the tip fall over two corresponding C atoms from the graphene sheet (see the black spheres in the structural model representing the tip atoms). The second case shows a honeycomb pattern due to the geometrical effects. Now, the atoms 1 and 2 are rotated with respect to the previous case, compensating the current difference between both maxima.

Figure 8(D) shows the I(Z) curves over a maximum and a minimum taken from figure 8(C). For a current of 0.8 nA (when the red line with open circles falls at 4.5 Å), the resulting corrugation is 0.15 Å, similar to the value obtained previously with the graphitic tip. Moving down the tip until we obtain the reference value of the gold tip, the corrugation slightly grows to 0.16 Å. This means that the corrugation is comparable to the one of the graphitic tip, showing a great improvement of both carbon tips with respect to the metallic tips.

3.2. Decorated tips

We now turn to discuss how the presence of adsorbates in the tip apex modifies the STM images. In particular, we shall

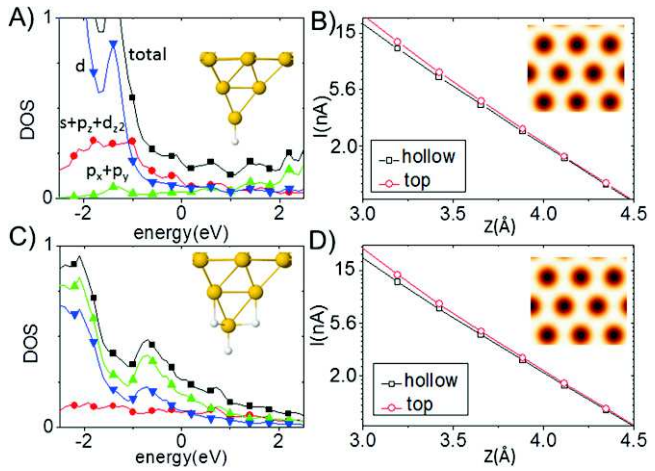

Figure 9. (A) Electronic DOS of the Au apex for a gold tip with a H atom adsorbed as shown in the inset. Black squares represent the total DOS of the gold apex, red circles are the $s + p_z + d_z^2$ orbitals, green up triangles correspond to $p_x + p_y$ orbitals and blue down triangles, the other four d orbitals. (B) I(Z) curves calculated over a C atom (red circles) and a hollow position (black squares) including the MS effects. In the inset, the image with the honeycomb pattern is shown. (C) and (D) the same for a gold tip with four H atoms bonded to the Au apex.

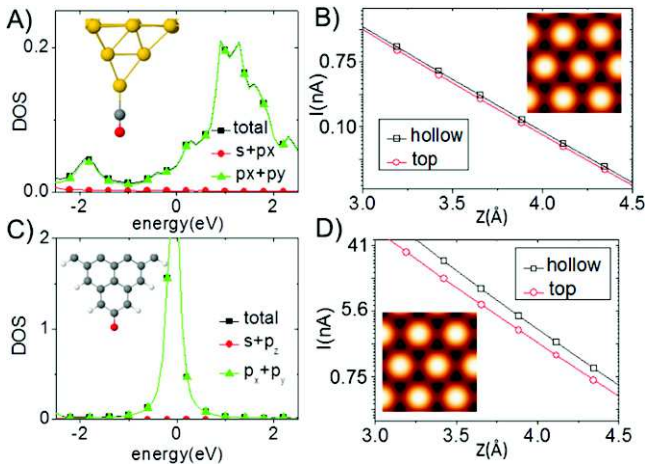

Figure 10. (A) Electronic DOS of the final O atom when a CO molecule is adsorbed in a gold tip as shown in the inset. Black squares represent the total DOS of the oxygen apex, red circles are the $s + p_z$orbitals and green up triangles correspond to $p_x + p_y$ orbitals. (B) I(Z) curves calculated over a C atom (red circles) and a hollow position (black squares) including the MS effects. In the inset, the resulting STM image with the triangular pattern is shown. (C) and (D) the same for a graphitic-like tip with an O atom replacing the last H atom.

focus our attention on the following examples: (i) adsorption of H atoms and CO molecules in the Au tip, (ii) substitution of the H apex of the graphitic tips by an O atom or an OH group, and (iii) presence of an O atom (or a OH group) in the diamond tips.

3.2.1. Metallic tips with H.. The adsorption of H_2 molecules below the metallic apex has been proposed as a mechanism to improve the image resolution in the experimental measurements [19, 20]. However, some of us proposed that what actually occurs is that H_2 molecules dissociate in the tip and the split H-atoms are then bound to the metallic atoms close to the apex [21]. The resulting tip is predicted to improve the image resolution, as suggested experimentally. Motivated by this work, we consider here the gold tip contaminated with one or four H atoms on the apex (see the inset in figures 9(A) and (C)). The H atoms do not have an important contribution to the DOS around the Fermi level, but they affect the distribution of the DOS of the Au apex. The most important contribution coming from the $s + p_z + d_z^2$ orbitals decreases with respect to the clean case, while the contribution of the p_x and p_y orbitals grows. Thus, a triangular contrast could be naively expected in the STM image. However, the simulated images show a honeycomb pattern for both tips as can be observed in the inset of figures 9(B) and (D), implying that the contribution to the tunnelling current of the directional $s + p_z + d_{z^2}$ is still higher than that of the other d or p orbitals. This effect can be explained in terms of the interaction between the tip-graphene orbitals ($T_{ST/TS}$ matrices in equation 1). The electronic hopping between the $s + p_z + d_z^2$ orbitals of the tip and the p_z orbital of the graphene is much higher than the one calculated for the p_x and p_y orbitals due to the higher directionality of the first orbitals. This is reflected in the final contribution to the current and consequently in the final image. In fact, the tip-sample interaction has a strong impact in the current as the $T_{ST/TS}$ matrices appears twice in equation 1. For this reason, although the DOS of $s + p_z + d_z^2$ and $p_x - p_y$ orbitals can be comparable, the final contribution to the current coming from the first kind of orbitals still results higher.

Now, we analyse the change in corrugation when the tip is contaminated with H atoms. For this purpose, we performed the I(Z) calculations over the hollow and top sites with both tips. The results are shown in figures 9(B) and (D) for the tip with one and four H atoms, respectively. The corrugation remains similar to the clean case for both tips: 0.025 Å at 4.5 Å. Now, the distance is defined by the last H atom and the tip should be moved 1.5 Å down in order to obtain the same current value as the one obtained with a clean tip at 4.5 Å. At this point, the corrugation grows to 0.06 Å for a tip with only one H-atom in the apex and to 0.07 Å when four atoms are joined to the final pyramid. These results are in good agreement with the improvement previously reported [21].

3.2.2. Tips contaminated with O, CO or OH atoms.. Following the experimental results of Gross *et al* [17, 18], we consider the gold tip modified by the adsorption of a CO molecule as an alternative way to improve the STM resolution. The molecular orbitals of CO are polarised towards the carbon atom [41]. Consequently, the carbon atom can easily accept electrons explaining its higher affinity to form bonds in the CO molecule. Our results confirmed this assumption, since the bond with the gold apex through the C atom is energetically more favourable than the one through the O atom. The corresponding structure is depicted in the

inset of figure 10(A). The simulated image is presented in the inset of figure 10(B) showing the characteristic maximum in the hollow site of the triangular pattern. As in the case of the first diamond tip, the result is explained in terms of the $p_x - p_y$ character of the DOS of the apex (in this case the O atom from the adsorbed CO molecule), as was previously reported [18] and as is shown in figure 10(A). Now the last Au atom is located at around 3 Å farther from the surface than the O atom and the dominant contribution comes from the p_x and p_y orbitals of the last O atom. Again, this effect can be explained in terms of the tip-sample interactions. The hopping decreases exponentially with the distance and for that reason, atoms with higher DOS but placed at larger distances can give a much lower contribution to the current than other closer atoms.

We now turn to the analysis of the corrugation obtained in the triangular images. Starting with the gold tip functionalized with the CO molecule, we calculate the I(Z) curves over the top and hollow sites (figure 10(B)) and estimate the corrugation for the higher current obtained at 4.5 Å, taking the same reference as with the clean metallic tip. Now, the computed current is around 20 pA and the corrugation obtained with this tip is 0.03 Å growing to 0.05 Å for a distance of 3.75 Å and a corresponding tunnelling current of 0.2 nA. At the initial distance of 4.5 Å, the first diamond tip mentioned in section 3.1.3 gives a corrugation of 0.08 Å. At this point, the current is higher than the Au + CO-tip case. Retracting the tip, the same current can be recovered at around 5.0 Å where the corrugation is almost unaltered (0.07 Å). Consequently, the diamond tip seems to produce a better triangular resolution than the gold tip with a CO molecule adsorbed.

As a next step, we investigate a CO-like apex in the graphitic tip by substituting the last hydrogen by an O atom (see the inset of figure 10(C)). As for the CO–Au tip, we observe an enhancement of the DOS and a p_x–p_y character (see figure 10(C)) that explains the formation of the maximum in the hollow position at the center of the hexagon in the simulated STM image. This is shown in the inset of figure 10(D). The corrugation obtained at 4.5 Å is 0.11 Å (see figure 10(D)), a higher value than for the two other tips but for a higher current (0.6 nA). Moving this tip back until a current of 0.2 nA is found (around 4.8 Å), the corrugation decreases to 0.10 Å still slightly higher than the diamond tip. Therefore, we can conclude that for low voltages the graphene-like tip with a O atom gives a higher triangular resolution than the other tips analysed in this work.

When an additional H atom is incorporated to the O apex, we obtain a similar behaviour as for the graphitic tip. Now, the bonds of the O atom are saturated producing a gap in the DOS. Consequently, only the same C atoms as in the graphitic tip contribute to the DOS at the Fermi level, as is shown in figure 11(A). As in the case of the pure graphitic tip, we have to rotate this tip in order to obtain the hexagonal pattern shown in the inset of figure 11(B). Similarly, the I(Z) curves have been calculated for a maximum and minimum site and they are shown in figure 11(B). As the tip-sample

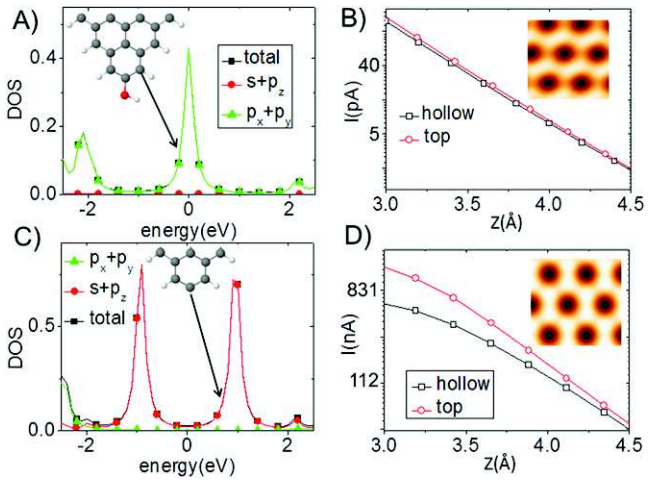

Figure 11. (A) Electronic DOS of the O atom when an OH group replaces the last H atom in the graphitic tip as shown in the inset. Black squares represent the total DOS of the oxygen apex, red circles are the $s + p_z$ orbitals and green up triangles correspond to the $p_x + p_y$ orbitals. (B) I(Z) curves calculated over a C atom (red circles) and a hollow position (black squares) including the MS effects. In the inset, the resulting STM image with the honeycomb pattern is shown. (C) and (D) the same for the graphitic tip when the last H atom is removed. The voltage applied in this case is −1.0 V.

distance is defined by the last hydrogen, the C-atoms contributing to the tunnelling current are located now at a larger distance than in the pure graphitic tip. For this reason, at 4.5 Å the same result is not recovered. The tip should be moved down 2 Å, where the OH group would be closer to the graphene sheet. For this reason, we consider the original graphitic tip as a better option.

In order to avoid the problem of the relative orientation of the tip with respect to the graphene sheet, we propose another interesting variation, which is displayed in the inset of figure 11(C). There, it can be observed that the original H atom has been removed from the graphitic apex. The resulting DOS of the last C atom is shown in figure 11(C) where two symmetric p_z levels appear at ±1 eV due to the unsaturated $p_z$orbital of the C apex associated to the lost bond. This orbital points in the normal direction to the surface. This results in a clear advantage, as the effect of the tip is the same for empty and filled states in the STM. As expected, the corresponding STM image presents a standard honeycomb pattern. In this case, we have increased the bias to −1 V in order to tunnel through the empty level located at 1 eV above the Fermi level. Again, the corrugation can be estimated from the calculated I(Z) when the tip is on a top or a hollow position. Now, the current at a tip-sample distance of 4.5 Å is 46 nA and the resulting corrugation is 0.05 Å. Interestingly, when the tip is approached to the graphene sheet, the saturation is found due to the MS effect, but there is a great increase on the corrugation instead of a contrast change. For example, at a tip-sample distance of 3.75 Å, the corrugation grows to 0.23 Å, much higher than the previous tips. However, this tip requires an ultra-high vacuum to be used, since it is expected to be very reactive and therefore able to catch whichever impurity is in the neighbourhood.

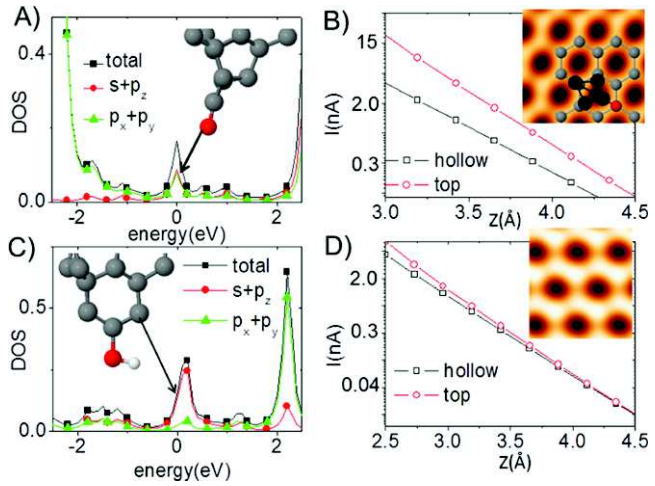

Figure 12. (A) Electronic DOS of the final O atom adsorbed in the diamond tip as shown in the inset. Black squares represent the total DOS of the oxygen apex, red circles are the $s + p_z$ orbitals and green up triangles correspond to $p_x + p_y$ orbitals. (B) I(Z) curves calculated over a C atom (red circles) and a hollow position (black squares) including the MS effects. In the inset, the resulting STM image with the honeycomb pattern is shown. (C) and (D) the same for a diamond tip with a OH atom replacing the last C atom.

Finally, we consider the diamond tips presented in figure 4 contaminated with an O atom. In the first case, (the structure of figure 4(A)) the O bonds with the final C atom forming a CO molecule that is desorbed from the tip. In the second case, the O is bonded again to the last C atom, but now forming a CO apex as shown in the inset of figure 12(A). The corresponding DOS of the adsorbed O atom is shown in the figure. Contrary to the other CO tips, the O atom presents in this case an important $s + p_z$ contribution. As a result, a honeycomb pattern is obtained in the calculated STM image (as shown in the inset of figure 12(B). The special atomic configuration of the tip produces a great current enhancement when it is placed near top positions. This is reflected in the corrugation extracted from the I(Z) curves of figure 12(B). It grows to 0.23 Å for a current of 0.09 nA obtained at 4.5 Å in the top position. This corrugation is much higher than the values obtained with the previous tips (growing even more for closer tip-graphene distance). We can conclude that this tip gives the best atomic resolution in the STM images among all the tips analysed in this work.

The last tip we would like to study is built by adsorbing a hydrogen atom onto the O atom of the previous tip. The atomic configuration is shown in the inset of figure 12(C), where the DOS is presented for the C-atom indicated. The OH group and the other two C-atoms do not provide an important contribution to the DOS around the Fermi level. On the contrary, the DOS of the C atom indicated with the black row has a $s + p_z$ character. Consequently, the resulting STM image has a hexagonal pattern, as shown in the inset of the (D) panel. The I(Z) curves reflect this behaviour in all the ranges investigated here. The corrugation is very small (0.02 Å) as well as the current (15 pA) at a tip-sample distance of 4.5 Å because the H atom is taken as the reference to define the tip height. Moving down the tip 2 Å, the current grows to 5 nA and the corrugation to 0.11 Å. Unfortunately, at this tip-graphene distance, the last atoms are located close to the graphene layer and an atomic reconstruction can be expected. For this reason, this tip cannot be considered as a good choice for the STM measurements.

4. Conclusions

In summary, we have presented a detailed theoretical analysis of the STM images produced by a great variety of tips using a graphene sheet as a test sample. In particular, the performance of standard metallic tips is compared with novel carbon-based tips to critically assess the usefulness of these latter ones for scanning tunnelling microscopy. In all cases, we have been able to explain the resulting STM images in terms of the complex interplay between the electronic properties and the atomic configuration of the tips and the electronic structure of the surface. From our analysis, we conclude that the carbon-based tips generally enhance the corrugation for both the triangular and honeycomb patterns commonly obtained. In particular, the diamond tip contaminated with an O atom gives the highest corrugation improving the resolution of the honeycomb pattern. The possible reactivity of this tip due to the last O atom is a disadvantage that can be solved by using the very stable graphitic tip. The best defined triangular shape was produced by the graphitic tip contaminated with an O atom where the $p_x + p_y$ contribution dominates. Our study clearly suggests that the use of a carbon-based tip can offer new possibilities for STM and it would be very interesting to extend this work to investigate the use of these tips to image other more complex structures.

Acknowledgments

C G P acknowledges funding by the Junta de Andalucía and the European Commission under the Co-funding of the 7th Framework Program in the People Program through the Andalucia Talent Hub program. J C C acknowledges financial support from the Spanish MINECO (Contract No. FIS2014–53488-P) and the Comunidad de Madrid (Contract No. S2013/MIT-2740).

References

[1] Binnig G and Rohrer H 1986 *IBM J. Res. Dev.* **30** 355
[2] González C *et al* 2004 *Phys. Rev. Lett.* **93** 126106
[3] Blanco J M *et al* 2005 *Phys. Rev.* B **71** 113402
[4] Liljeroth P, Swart I, Paavilainen S, Repp J and Meyer G 2010 *Nano Lett.* **10** 2475
[5] Tseng T-C *et al* 2010 *Nature Chem.* **2** 374
[6] Majzik Z, Drevniok B, Kaminski W, Ondraacek M, McLean A B and Jelínek P 2013 *ACS Nano.* **7** 2686
[7] Tersoff J and Hamman D 1983 *Phys. Rev. Lett.* **50** 1998
[8] Tersoff J and Hamman D R 1985 *Phys. Rev.* B **31** 805
[9] Chen C J 1990 *Phys. Rev. Lett.* **65** 448

[10] Mingo N, Jurczyszyn L, García-Vidal F J, Sainz-Pardo R, de Andreés P L, Flores F, Wu S Y and More W 1996 *Phys. Rev.* B **54** 2225
[11] Cerdá J, Van Hove M A, Sautet P and Salmeron M 1997 *Phys. Rev.* B **56** 15885
[12] Hofer W A 2003 *Prog. Surf. Sci.* **71** 147
[13] Li Z, Schouteden K, Iancu V, Janssens E, Lievens P, Van Haesendonck C and Cerda J I 2015 *Nano Research* **8** 2223
[14] Sánchez-Sánchez C *et al* 2010 *Nanotechnology* **21** 405702
[15] Bartels L *et al* 1998 *Phys. Rev. Lett.* **80** 2004
[16] Meyer G, Bartels L and Rieder K-H 2001 *Comp. Mat. Sci.* **20** 443
[17] Gross L, Mohn F, Moll N, Liljeroth P and Meyer G 2009 *Science* **325** 1110
[18] Gross L, Moll N, Mohn F, Curioni A, Meyer G, Hanke F and Persson M 2011 *Phys. Rev. Lett.* **107** 086101
[19] Weiss C, Wagner C, Kleimann C, Rohlfing M, Tautz F S and Temirov R 2010 *Phys. Rev. Lett.* **105** 086103
[20] Weiss C, Wagner C, Temirov R and Tautz F S 2010 *J. Am. Chem. Soc.* **132** 11864
[21] Martínez J I, Abad E, González C, Flores F and Ortega J 2012 *Phys. Rev. Lett.* **108** 246102
[22] Cheng Z, Du S, Guo W, Gao L, Deng Z, Jiang N, Guo H, Tang H and Gao H-J 2011 *Nano Res.* **4** 523
[23] Grushko V *et al* 2014 *Nanotechnology* **25** 025706
[24] Ohmori T, Nagahara L A, Hashimoto K and Fujishima A 1994 *Rev. Sci. Instrum.* **65** 404
[25] Colton R, Baker S, Baldeschwieler J and Kaiser W 1987 *Appl. Phys. Lett.* **51** 305
[26] Rohlfing D and Kuhn A 2007 *Electroanalysis* **19** 121
[27] Castellanos-Gomez A, Agraït N and Rubio-Bollinger G 2010 *Nanotechnology* **21** 145702
[28] Dappe Y J, González C and Cuevas J C 2014 *Nanoscale* **6** 6953
[29] Kichin G, Wagner C, Tautz F S and Temirov R 2013 *Phys. Rev.* B **87** 081408
[30] Ondrácek M *et al* 2011 *Phys. Rev. Lett.* **106** 176101
[31] Keldysh L V 1964 *Zh. Eskp. Teor. Fiz.* **47** 1515
Keldysh L V 1965 *Sov. Phys. JEPT* **1018**
[32] Blanco J M, Flores F and Pérez R 2006 *Prog. Surf. Sci.* **81** 403
[33] Lewis J P *et al* 2011 *Phys. Status Solidi* B **248** 1989
[34] Basanta M A, Dappe Y J, Jelinek P and Ortega J 2007 *Comput. Mater. Sci.* **39** 759
[35] Sankey O F and Niklewski D J 1989 *Phys. Rev.* B **40** 3979
[36] Castro Neto A H, Guinea F, Peres N M R, Novoselov K S and Geim A K 2009 *Rev. Mod. Phys.* **81** 109
[37] Wallace P R 1947 *Phys. Rev.* **71** 622
[38] Bena C and Kivelson S A 2005 *Phys. Rev.* B **72** 125432
[39] Xu K, Cao P and Heath J R 2009 *Nano Lett.* **9** 4446
[40] Horcas I, Fernández R, Gómez-Rodríguez J M, Colchero J, Gómez-Herrero J and Baró A M 2007 *Rev. Sci. Instrum.* **78** 013705 WSxM solutions website www.wsxmsolutions.com
[41] Föhlisch A *et al* 2000 *Phys. Rev. Lett.* **85** 3309